www.vbripress.com, www.amlett.com, DOI: 10.5185/amlett.2012.4330 Published online by the VBRI press in 2012

Nanaostructured ZnO, ZnO-TiO_2 and ZnO-Nb_2O_5 as solid state humidity sensor

Richa Srivastava[1] and B. C. Yadav[1,2*]

[1]*Nanomaterials and Sensors Research Laboratory, Department of Physics, Lucknow University, Lucknow 226007, U. P., India*

[2]*Department of Applied Physics, School for Physical Sciences, Babasaheb Bhimrao Ambedkar University, Lucknow 226025, U.P., India*

[*]Corresponding author. Tel: (+91) 9450094590; Fax: (+91) 522-4060185; E-mail: balchandra_yadav@rediffmail.com

Received: 16 April 2012, Revised: 02 May 2012 and Accepted: 05 May 2012

ABSTRACT

Present paper deals with a comparative performance of n-type ZnO, ZnO-TiO_2 and ZnO-Nb_2O_5 nanomaterials as humidity sensors. ZnO was synthesized through hydroxide route. TiO_2 and then Nb_2O_5 were used as additives for improvement of sensitivity. Scanning electron micrograph of ZnO shows rod-like particles with average diameter 40 nm. Structural properties by X-Ray diffraction were studied. The minimum crystallite sizes of ZnO-TiO_2 and ZnO-Nb_2O_5 calculated from Scherrer's formula were found to be 19 and 17 nm respectively. The pellet of each sensing material was annealed at temperatures 150, 300, 450 and 550 °C for 3 h and checked for its sensing efficiency. Each heat treated pellet was exposed to humidity under controlled condition and variations in resistance with the humidity were recorded. Comparative study of sensitivities of each sensing element was performed. Average sensitivity achieved was 8 MΩ/%RH for the n-type ZnO annealed at 550 °C. After chemical mixing of TiO_2, the sensitivity increased to 18 MΩ/%RH and after Nb_2O_5, it was found to be 19 MΩ/%RH. Activation energy of electrical transport and Kelvin radii of each sensing elements were also studied. Copyright © 2012 VBRI Press.

Keywords: Humidity; sensitivity; nanostructures; resistance; surface morphology.

Richa Srivastava has received her B.Sc. degree in 2001, M.Sc. degree in 2003 and Ph. D. degree in 2008 from Lucknow University, Uttar Pradesh, India. Currently she is Post-Doctoral fellow in Physics Department, University of Lucknow, Lucknow. She is also awarded by prominent G.C. Jain Memorial prize for Best Thesis in Material Science-2009 instituted by the Material Research Society of India. She has published sixteen research papers in reputed international journals and thirty research papers in conference proceedings. Her current interests of research are synthesis and characterization of nanomaterials and their applications as sensors, thin and thick film sensors, humidity sensors, gas sensors, Temperature and optical sensors etc.

B. C. Yadav has received his B.Sc. and M. Sc. Degrees from Dr. R. M. L. Avadh University, Faizabad, Uttar Pradesh, India in the years 1991 and 1993 respectively. He obtained his Ph.D. degree in year 2001 from Department of Physics, University of Lucknow, and Uttar Pradesh, India. Currently he is an Associate Professor in the Department of Applied Physics, School for Physical Sciences in the Babasaheb Bhimrao Ambedkar University, Lucknow. He is recipient of prestigious Young Scientist Award-2005 instituted by the State Council of Science and Technology. Dr. Yadav has worked as International Brain Pool Fellow at Korea Research Institute for Chemical Technology, Daejeon, South Korea. He has published more than sixty research/review papers in reputed international journals. His current interests of research are in synthesis of metal oxides nanoparticles, metallopolymers, nanocomposites, carbon nanotubes etc., characterizations and their applications as sensors, thin and thick film sensors, pressure sensor, glucose sensors etc.

Introduction

Effect of humidity on various materials is well known for a long time in many ways. It affects mankind directly or indirectly. The irreversible effect due to humidity eventually causes permanent damage to the exposed surfaces. Therefore, there is an urgent need to measure and control precisely the humidity in various environments [**1**]. At the same time the reversible effect of humidity on materials may be exploited for the measurement of humidity. Most of the humidity sensors based on metal oxide show good sensitivity over the entire range of %RH. Nano sized zinc oxide due to the large band gap 3.37 eV and high exciton binding energy of 60 meV shows various useful properties and gives large and diverse range of growth of different type of morphologies such as nanosheets, nanocombs, nanobelts, nanowires and nanorings, which may be used in various applications [**2-4**].

It is one of the promising materials among metal oxides for use in humidity sensors [**5-10**] and gas sensors [**11-18**].

We have tried to emphasize the synergistic role of the doping materials in the preparation of excellent humidity sensor. Doping is an attractive and effective tool for maneuvering different properties such as better sensitivity, good reproducibility, and linear characteristics with humidity [**19-23**]. The behavior of TiO_2 is such that it remains stable over the time and thermal cycling when it is exposed to the various chemical species, likely to be present in the ambient to be sensed. Nb_2O_5 is easily available at the lower cost. It is a ceramic material and appears as white crystals or powder. It has stable electrical parameters. Both TiO_2 and Nb_2O_5 are very sensitive to humidity [**24-37**].

Owing to the useful properties of TiO_2 and Nb_2O_5, each of these materials has been chemically mixed separately with ZnO nanomaterial for improvement of sensitivity, reproducibility and linear characteristics with humidity, which would be very useful for vast area of potential application in different type of electronic devices.

In this paper synthesized n-type ZnO, ZnO-TiO_2 and ZnO-Nb_2O_5 as sensing materials were characterized using SEM and XRD and a comparative study of their humidity sensing behaviors were made.

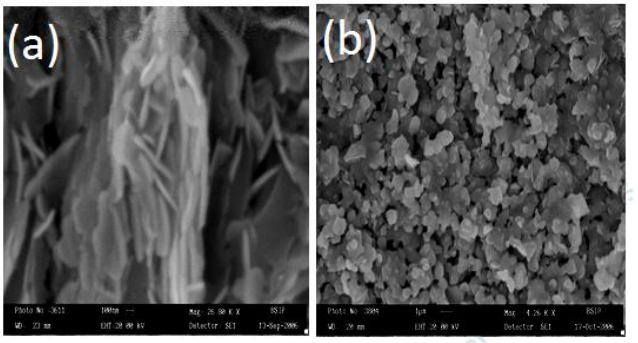

Fig. 1. Scanning electron micrographs of ZnO nanomaterial in the form of pellet prepared (a) at room temperature in nanoscale (b) at 550 ºC in microscale.

Experimental

Synthesis of material

ZnO was prepared by conventional precipitation method by adding sodium hydroxide solution to zinc sulphate solution (1:2.2) using 'sudden drop method' [**38**] under vigorous stirring. After completion of reaction, it was kept for 3 days and then filtered and washed with deionized water to remove sodium and other ions. Subsequent heat treatment of precipitate at 550 ºC for 3 h gave zinc oxide in powder form.

For synthesis of ZnO-TiO_2 and ZnO-Nb_2O_5 nanocomposite materials, TiO_2 powder (99.58%, Qualigens) and Nb_2O_5 (99.25%, Johnson & Matthey Co. Ltd, London) were homogeneously mixed in the ratio 1:4 by weight with synthesized zinc oxide within isopropyl alcohol (50 ml) as solvent separately. After vigorous stirring of 10 h, these were filtered out and dried. After that, zinc titanium oxide (Zn_2TiO_4) and zinc niobium oxide ($ZnNb_2O_6$) composite materials in the form of powders were obtained.

The pellets of identical dimensions (10 mm in dia and 4 mm in thickness) of these materials were made by using hydraulic pressing machine (KBR Press, Germany) under the pressure 30 MPa at room temperature. Each pellet was annealed at temperatures 150, 300, 450 and 550 °C for 3 h and used as humidity sensors.

Each pellet was kept within an electrode holder and has been exposed to humidity in the self-designed humidity chamber. Variations in resistance with humidity were recorded by using a digital multimeter (VC 9808, India). Relative humidity is measured using digital hygrometer. The least count of Hygrometer used here is 1% RH.

Characterization of n-type ZnO, ZnO-TiO_2 and ZnO-Nb_2O_5

The morphology of sensing material in the form of pellet was investigated with a scanning electron microscope (SEM, LEO-0430 Cambridge). **Fig. 1a** shows SEM of ZnO in the form of nanorods with a length of around 250-350 nm and average diameter between 40-50 nm and another SEM of ZnO calcined at 550 °C is shown in **Fig. 1b**. It shows uniform distribution of pores with clusters of crystallites over the entire surface of the material. **Fig. 2** and **Fig. 3** show SEMs of ZnO-TiO_2 and ZnO-Nb_2O_5 in the form of pellets prepared at room temperature respectively. They show porous nature of sensing materials with different crystallite sizes.

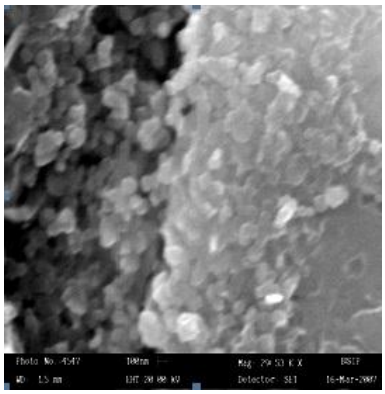

Fig. 2. Scanning electron micrograph of ZnO-TiO_2 nanomaterial prepared at room temperature.

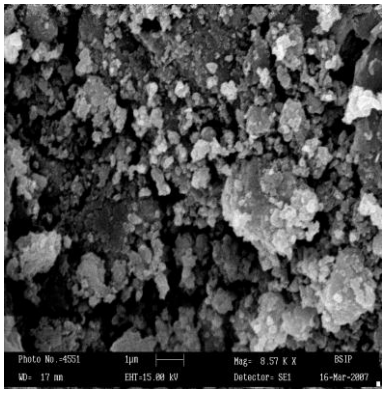

Fig. 3. Scanning electron micrograph of ZnO-Nb_2O_5 nanomaterial prepared at room temperature.

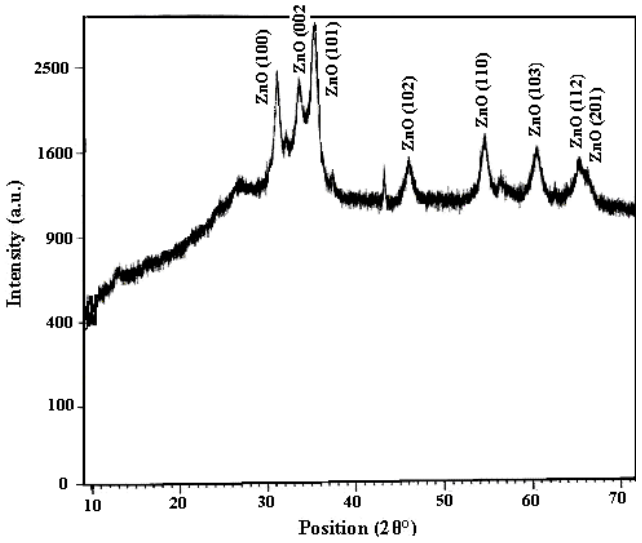

Fig. 4. X-Ray Diffraction of sensing material in the form of ZnO powder annealed at 550 ºC.

X-Ray diffraction system (X-Pert, PRO, Netherland) with Cu-K_α source radiation having wavelength 1.54 Å was used for the characterization of the sample. The X-Ray diffraction patterns obtained show the extent of crystallization and the crystallite sizes of sensing materials were calculated using Scherrer's formula. **Fig. 4, 5** and **6** show X-ray diffraction patterns of ZnO, ZnO-TiO_2 and ZnO-Nb_2O_5 in the form of powder. Major phase of ZnO exists for 2θ = 36˚ at the plane (101) as shown in **Fig. 4**. The average crystallite size of ZnO as calculated is 40 nm.

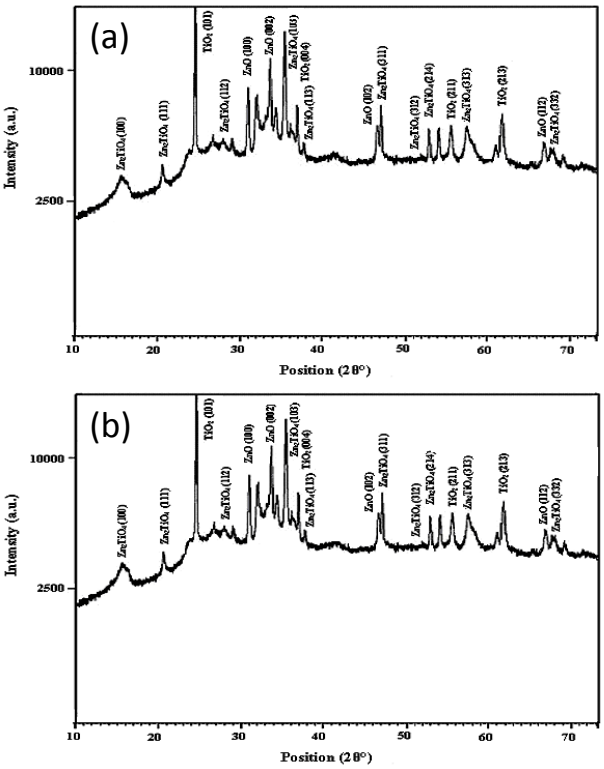

Fig. 5. X-Ray Diffraction of sensing material in the form of ZnO-TiO_2 prepared (a) at room temperature and (b) at 550 ºC.

Fig. 5a shows the XRD pattern of sensing materials in the form of ZnO-TiO_2 powder at room temperature. At this temperature sample contains $ZnTiO_3$ at the plane (024) for 2θ = 48˚. The FWHM and d-spacing corresponding to this peak are 0.134° and 1.8936 Å respectively. Unidentified peaks are attributed to impurities of $ZnSO_4$ and other ions. The minimum crystallite size was 19 nm as per calculation.

Fig. 6a shows XRD pattern of sensing material prepared at room temperature and it reveals that the sample contains $Zn_3Nb_2O_8$ and some quantity of ZnO, $Na_2Nb_2O_6$ with impurities of $ZnSO_4$. The minimum crystallite size of synthesized material $Zn_3Nb_2O_8$ at room temperature 19°C was found as 17 nm. The corresponding values of 'd' spacing and FWHM of sensing material are 1.37 Å and 0.0614˚ respectively at the plane (812) for 2θ = 68˚.

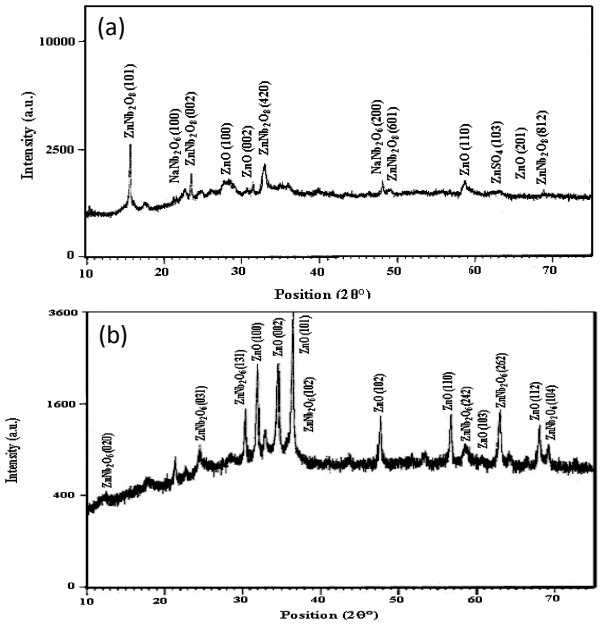

Fig. 6. X-Ray Diffraction of sensing material in the form of ZnO-Nb_2O_5 powder prepared (a) at room temperature and (b) at 550 ºC.

Effects of annealing on XRD patterns of sensing materials of ZnO-TiO_2 and ZnO- Nb_2O_5 were also studied as shown in **Fig. 5b** and **6b** respectively. **Fig. 5b** shows the X-Ray diffraction pattern of sensing material annealed at 550˚C in the powder form. It shows that the sample contains zinc titanium oxide (Zn_2TiO_4). FWHM for this peak is 0.110˚ and d-spacing is 2.33 Å. Most of the peaks are identified as Zn_2TiO_4. **Fig. 6b** shows the XRD pattern of sensing material annealed at temperature 550 ºC. Zinc niobium oxide nanomaterial ($ZnNb_2O_6$) was obtained after annealing the sample at temperature 550 ºC and can be seen by X-Ray diffraction pattern. Major phase of $ZnNb_2O_6$ sensing material has been observed corresponding to the values of 'd' spacing 1.38 Å and FWHM 0.230˚ at the planes (104) for 2θ = 68˚.

Measurements of humidity sensing properties

Experimental set up reported earlier [**39**] was used for this investigation and is shown in **Fig. 7(a)**. The humidifier/dehumidifier was kept in a dish over a stand. Variations in %RH were measured with the help of

hygrometer (Huger, Germany) and variations in resistance were measured using digital multimeter (VC 9808, CE, India). The temperature of the chamber remained the same throughout the observations. The chamber was then dehumidified up to 10%RH using saturated solution of potassium hydroxide. The prepared pellet of sensing material was put within a conductivity-measuring holder having Cu electrode-pellet-Cu electrode arrangement as shown in **Fig. 7(b)**. The humidity chamber was humidified using saturated solution of potassium sulphate in deionized water. It was observed that as %RH inside the chamber increases from 10-95%RH, resistance of the sensing material decreases over the entire range of RH. Further the pellet, which acts as sensing material was annealed for 3 h at 150, 300, 450 and 550 °C in an electric furnace successively. After each step annealing, the pellet was exposed to humidity and variations in resistance with humidity were observed.

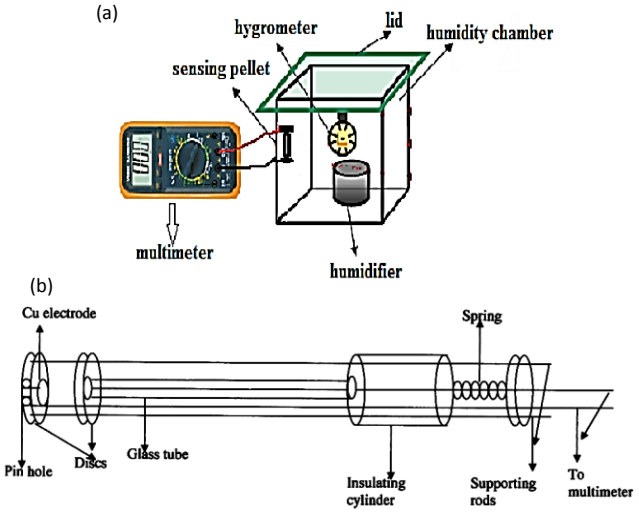

Fig. 7. (a) Experimental set-up and (b) Conductivity measuring holder.

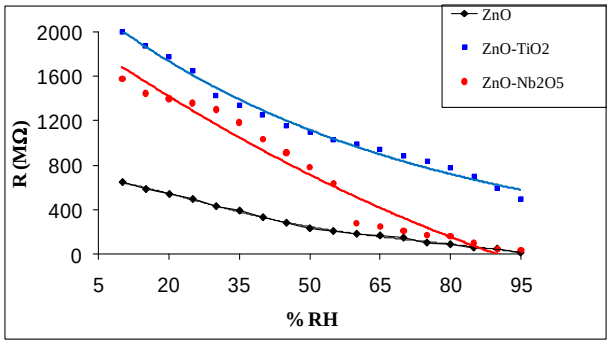

Fig. 8. Variations in resistance with the variations in relative humidity for the sensing elements made of ZnO, ZnO-TiO_2 and ZnO-Nb_2O_5 respectively.

Study of sensitivity

Sensitivity of humidity sensor has been defined as the change in resistance (ΔR) of the sensing element per unit change in %RH and is given below –

$$S = \frac{\Delta R}{\Delta \%RH}\ M\Omega/\%RH \quad \text{----------(1)}$$

The sensitivities of sensors using ZnO, ZnO-TiO_2 and ZnO-Nb_2O_5 were studied at different annealing temperatures but reported only which corresponds to highest point of average sensitivity. Maximum average sensitivity of zinc oxide based humidity sensor was achieved at annealing temperature 550 °C. Variations in resistance with the %RH for ZnO, ZnO-TiO_2 and ZnO-Nb_2O_5 sensing elements were plotted in **Fig. 8**. The comparative chart of average sensitivity for each sensing element is depicted in **Table 1**.

Table 1. Variations in average sensitivity with different sensing elements.

Sensitivity for range of %RH / Sensing Elements	10-20	20-30	30-40	40-50	50-60	60-70	70-80	80-95	Average Sensitivity (MΩ/%RH) From 10-95%
n-type ZnO	10.8	11.0	10.0	10.0	5.0	3.5	6.0	5.0	7.66 ≈ 8
ZnO-TiO_2	22.3	34.7	17.8	15.0	10.6	10.6	11.3	18.87	17.65 ≈ 18
ZnO-Nb_2O_5	17.6	9.7	26.7	25.3	50.5	6.8	5.0	8.67	18.78 ≈ 19

Study of activation energy

The resistance-temperature plot of ln(R) vs 1/T, known as Arrhenius plot, has a slope of E_a/k according to Eq. $R = R_o e^{Ea/kT}$. The slope of a linear zone gives the activation energy (E_a) for electrical transport of charge carriers in semiconducting materials can be calculated [**10**]. From our experiments we studied R-T characteristics of each sensing elements and found that ZnO-Nb_2O_5 nanomaterial gave maximum slope which is shown in **Fig. 9**.

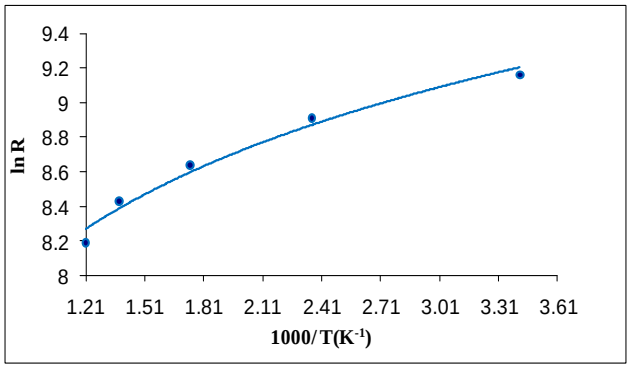

Fig. 9. Arrhenius Plot for the sensing element made of ZnO-Nb_2O_5.

Activation energy calculated from Arrhenius plots of sensing materials was found to be maximum 0.029 eV for ZnO-Nb_2O_5 in the range 19-300 ºC. Variations in activation energy for ZnO, ZnO-TiO_2 and ZnO-Nb_2O_5 at 19-300 °C are depicted in **Table 2**.

Table 2. Variations in activation energies with different sensing materials.

Sensing materials	Activation energy (eV)
n-type ZnO	0.0041
ZnO-TiO_2	0.012
ZnO-Nb_2O_5	0.029

Study of kelvin radii

The radii of the pores in a porous material known as Kelvin radii can be calculated by Kelvin equation given as under:Where γ = Surface tension of water, M = Molecular weight of water, P/ P_s = Relative Humidity, ρ = Density of water and r_K is Kelvin radii.

$$r_K = \frac{2\gamma M}{\rho RT \ln(P_s / P)} \text{ ----------(2)}$$

At the time of investigations of solid-state humidity sensor, the relation between humidity sensing properties and porosity were studied. Shimizu et al [**40**] gave theoretical interpretation of this correlation. Later on, others [**41**] followed it. There are various methods to determine the pore size distribution [**42**]. Kelvin radii for ZnO, ZnO-TiO_2 and ZnO-Nb_2O_5 were evaluated and it was found that each sensing element possesses the same value of Kelvin radii corresponds to each value of relative humidity as shown in **Fig. 10**. From characteristics, it was observed that as relative humidity increases, Kelvin radius increases. In lower humidity region chemisorptions occur at atomic level and increase in humidity causes physisorption. Ultimately it converts in to condensation through larger capillary pores. Some additional pores will be filled by water vapour which increases the pore size markedly.

Results and Discussion

For all sensing elements, i.e. ZnO, ZnO-TiO_2 and ZnO-Nb_2O_5, **Fig. 8** clearly reflects that as %RH increases, resistance decreases from 10 to 95%. The curve for the sensing element of ZnO shows that as RH increases, resistance decreases sharply up to 50%RH and shows highest sensitivity in this range followed by a less rapid decrease up to 95%RH as relative humidity increases. Average sensitivity 8 MΩ/%RH over the entire range of relative humidity was achieved. The curve for the sensing element ZnO-TiO_2 prepared at room temperature shows that as RH increases, resistance decreases up to 95%RH and there are two linear dependence regions: first region from 10 to 30%RH having average sensitivity 25 MΩ/%RH and second from 30 to 95%RH was having 11 MΩ/%RH. This plot shows better linear response of the sensor and highest average sensitivity 18 MΩ/%RH was achieved. Curve for ZnO-Nb_2O_5 sensing element shows that as RH increases, resistance decreases markedly up to 65%RH which gives maximum slope having maximum average sensitivity 23 MΩ/%RH. It decreases slowly in the range 65-95% and maximum average sensitivity 19 MΩ/%RH over the entire range of %RH was achieved.

The adsorption of moisture through ceramic oxide surfaces can be understood as follows: adsorptions of moisture affect the protonic conduction on the surface and the conductivity varies with amount of the water they adsorb. This principle is employed for the measurement of humidity in resistive-type humidity sensors. Ceramic humidity sensors show chemical resistance [**43-45**]. The change in impedance of porous ceramics at different environmental humidity levels is related to the mechanism of water adsorption on the oxide surface.

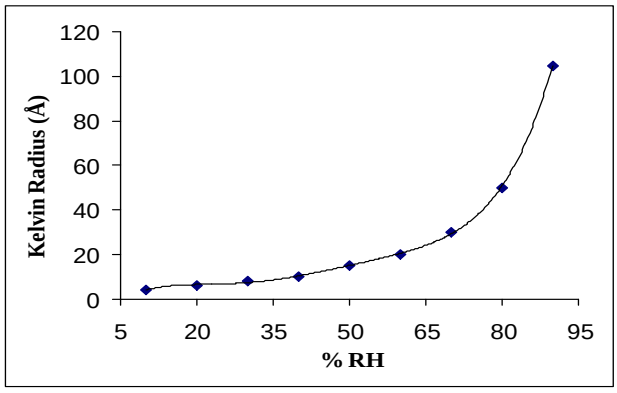

Fig. 10. Variations of Kelvin radii (Å) against relative humidity at room temperature.

At the initial stage of adsorption, the negatively charged oxygen is electro-statically attached to the positively charged metallic ions of the sensor material to form hydroxides. Thus the grain surfaces, which are contiguous to the pores, are covered by a chemisorbed monolayer. As relative humidity increases, first physisorbed layer localized by hydrogen bonding of a single water molecule to two surface hydroxyls is set up. A hydronium group H_3O^+ is thereafter formed through those molecules in the second layer that are on the average singly hydrogen bonded to the underlying layer as shown in **Fig. 11.**

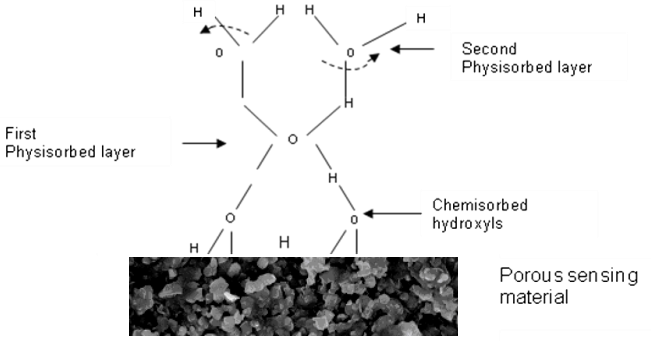

Fig. 11. Sensing mechanism of solid state humidity sensor.

Thus a proton is released to neighbouring water molecules which accept it while releasing another proton and so on (Grotthuss chain reaction mechanism). This proton moves freely along the water and thus determines the sensor conductivity. At higher humidity levels, liquid water condenses in the pores and electrolytic conduction occurs simultaneously with protonic transport.

The variations in sensitivities in MΩ/%RH of sensing elements made of ZnO, ZnO-TiO_2 and ZnO-Nb_2O_5 for each interval of 10%RH have been shown in Table 1. It could be observed that after chemical mixing of TiO_2, sensitivity of ZnO increases more than two times i.e. 18 MΩ/%RH and after mixing of Nb_2O_5, the highest sensitivity so achieved was 19 MΩ/%RH for the entire range of RH. ZnO-Nb_2O_5 sensing material was much porous and amorphous at room temperature. A close look at scanning electron micrographs reveals that latter one was more porous in comparison to others (ZnO and ZnO-TiO_2). Therefore the maximum value of sensitivity (19 MΩ/%RH) was achieved for this material.

X-Ray diffraction patterns of powdered samples show crystalline nature of pure zinc oxide. After mixing of TiO_2 and Nb_2O_5, it became less crystalline with increased number of pores and hence enhanced sensitivities were achieved for these materials.

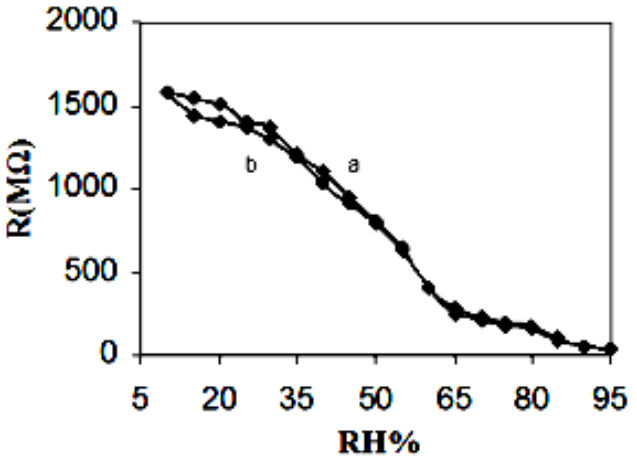

Fig. 12. Reproducibility of result for the sensing element ZnO-Nb_2O_5.

Reproducibility of results for all sensing elements were checked and found that ZnO-Nb_2O_5 sensing element has better reproducibility with 5% hysteresis than others. The curve for reproducibility of result is shown in **Fig. 12**. Curve 'a' shows linear decrease in resistance with increasing %RH and curve 'b' shows increase in resistance of sensing material with decreasing %RH reversibly.

Conclusion

In order to develop highly efficient humidity sensor, nanostructured zinc oxide has been doped with TiO_2 and Nb_2O_5 and a detailed study has been performed which is very useful for measuring and monitoring the relative humidity of environment at room temperature. ZnO-Nb_2O_5 nanocomposite material prepared at room temperature gave nanocrystallites having minimum size 17 nm which has good sensing properties for water vapour. Highest average sensitivity 19 MΩ/%RH has been achieved over the entire range from 10 to 95% at room temperature. Results are found to be reproducible and no ageing effects have been observed for five months. Thus humidity sensor made of ZnO-Nb_2O_5 based on electrical resistance is cost effective, easy to fabricate and user friendly and can be used for both indoor and outdoor applications for entire range of the %RH.

Acknowledgement

Corresponding author is thankful to Department of Science and Technology, India for financial support in the form of FAST-TRACK project (SR/FTP/PS-21/2009). Dr. Richa Srivastava is highly grateful to University Grants commission, Delhi for 'Post Doctoral Fellowship' (No.F.15-79/11 (SA-II)). We are also thankful to Dr. C.D. Dwivedi, Retd. Scientist 'F', D.M.S.R.D.E. Kanpur, U.P., for fruitful discussions.

Reference

1. Ruskin, R. E. *Humidity and Moisture*, Reinhold, **1965**, Vol. 1.
2. Feng, X.; Ke, Y.; Guodong, L.; Qiong, L.; Ziqiang, Z. *Nanotech.* **2006**, *17*, 2855. **DOI:**10.1088/0957-4484/17/12/005
3. Wei, Q.; Meng, G.; An, X.; Hao Y.; Zang, L. *Nanotech.*, **2005**, *16*, 2561. **DOI:**10.1088/0957-4484/16/11/016
4. Kim, C.; Chun, M. J.; Kim, D.E. *Nanotech.*, **2005**, *16*, 2104.
5. Shukla, S. K.; Parashar, G. K.; Misra, P.; Yadav, B. C.; Shukla, R. K.; Bali, L. M., Dubey, G. C. *Sens. Actuators B, 2004*, Vol.98, No.1, Issue 1, 5. **DOI:** 10.1016/j.snb.2003.05.001
6. Zhou, X.; Jiang, T.; Zhang, J.; Wang, X.; Zhu, Z. *Sens. Actuators B*, **2007**, *123* 299. **DOI:** 10.1016/j.snb.2006.08.034
7. Kavasoglu, N.; Bayhan, M. *Turk. J. Phys.*, **2005**, *29*, 249.
8. Wan, Q.; Li, Q.H.; Chen, Y. J.; Wang, T. H.; He, X. L.; Gao, X. G; Li, J. P. , *App. Phys. Lett.*, **2004**, 84, 3085. **DOI:** 10.1063/1.1707225
9. Zhang, Y.; Yu, K.; Ouyang, S.; Luo, L.; Hu, H.; Zhang Q.; Zhu, Z. *Physica B: Cond. Matt.* **2005**, *368*, 94. **DOI:** 10.1016/j.physb.2005.07.001
10. Yadav, B. C.; Srivastava, R.; Dwivedi, C. D., Pramanik, P. *Sens. Actuators B*, **2008**, *131*, 216. **DOI:** 10.1016/j.snb.2007.11.013
11. Rout, C. S.; Harikrishna, S; Vivekchand, S. R. C.; Govindaraj, A.; Rao, C. N. R. *Chem. Phy. Lett.* **2006**, *418*, 584. **DOI:** 10.1016/j.cplett.2005.11.040
12. Lim, H. J.; Lee, D. Y.; Oh, Y. J. *Sens. Actuators A*, **2006**, *125*, 405. **DOI:** 10.1016/j.sna.2005.08.031
13. Sun, Z. P.; Liu, L.; Zhang L.; Jia, D. Z. *Nanotech.* **2006**, *17*, 2266. **DOI:** 10.1088/0957-4484/17/9/032
14. Yadav, B. C.; Srivastava, R.; Yadav, A. *Sensors & Materials*, **2009**, *21*, 87.
15. Yadav, B. C.; Srivastava, R.; Yadav, A.; Srivastava, V. *Sensor Letters*, **2008**, *5*, 714. **DOI:** 10.1166/sl.2008.m132
16. Wu, N.; Zhao, M.; Zheng, J. G.; Jiang, C., Myers, B.; Le, S.; Chyu, M.; Mao, S. X. *Nanotech.* **2005**, 16, 2878. **DOI:** 10.1088/0957-4484/*16*/12/024
17. Zhang, Q.; Xie, C.; Zhang, S.; Wang, A.; Zhu, B.; Wang, L.; Yang, Z. *Sens. Actuators B*, **2005**, *110*, 370. **DOI:** 10.1016/j.snb.2005.02.017
18. Shinde, V. R.; Gujar, T. P.; Lokhande, C. D. *Sens. Actuators B*, **2007**, *120*, 551. **DOI:**10.1016/j.snb.2006.03.007
19. Shukla, Tripti; Yadav B. C.; Tandon, P. *Sensor Letters*, Vol. 9, No. 2, **2011**, 533. **DOI:** 10.1166/sl.2011.1508
20. Yadav, B. C.; Yadav, R. C.; Dwivedi P. K. *Sensors & Actuators: B. Chemical*, **2010**, *148*, 413. **DOI:** 10.1016/j.snb.2010.05.046
21. Barakat, M. A.; Hayes, G.; Shah, S. I. *J. Nanosci. Nanotech.* , **2005**, *5*, 759.
22. Su, P. G.; Wang, C. P.; *Sens. Actuators B*, **2008**, *129*, 538.
23. Yadav, B. C.; Srivastava R.; Dwivedi; C. D. *Phil. Magazine* 88, **2008**, *7*, 1113. **DOI:** 10.1080/14786430802064642
24. Cantalini, C.; Pelino, M. *J. Am. Ceram. Soc.* **1992**, *75*, 546.
25. Yadav, B. C.; Pandey, N. K.; Srivastava, A. K.; Sharma P. *Meas. in Sc. & Tech.* **2007**, *18*, 1.
26. Yadav, B. C.; Shukla, R. K.; *Indian J. Pure App. Phy.* **2003**, *32*, 13.
27. Montesperelli, G.; Pumo, A.; Traversa, E.; Gusmano, G.; Bearzotti, A.; Montenero, A.; Gnappi, G. *Sens. Actuators B*, **1995**, *24*, 705. **DOI:**10.1016/0925-4005(95)85156-9
28. Ying, J.; Wan, C.; He, P. *Sens. Actuators B*, **2000**, *62*,165.
29. Tai, W. P.; Kim, J. G.; Oh, J. H.; Kim, Y. S. *Sens. Actuators B* **2005**, *105*, 925.
30. Bearzotti, A;. Bianco, A.; Montesperelli, G.; Traversa, E. *Sens. Actuators B*, **1994**, *18*, 525.
31. Faia, P. M.; Furtado, C. S.; Ferreira, A. J. *Sens. Actuators B* 101, **2004**, *1*, 183. **DOI:** 10.1016/j.snb.2004.02.050

32. Yadav, B. C.; Shukla, R. K.; Bali, L. M. *Indian J. of Pure App. Phy*. **2005**, *43*, 51.
33. Yadav B. C., *Sens. Trans. J.* **2007**, 79, 1217.
34. Kurioka, N.; Watanabe, D.; Haneda, M.; Shimanouchi, T.; Mizushima, T.; Kakuta, N.; Ueno, A.; Hanaoka, T.; Sugi, Y. *Catal. Today* **1993**, *16*, 495.
35. Yadav, B. C.; Srivastava, R.; Singh, M.; Kumar R.; Dwivedi, C. D. *Sens. Trans. J.* **2007**, *85*, 1765.
36. Samuel, V.; Gaikwad A. B.; Ravi, V. *Bull. Mater. Sci.* **2006**, *29*, 123.
DOI: 10.1007/BF02704604
37. Dwivedi, C. D. Studies on ageing of alumina by X-Ray diffraction, Society of Chemical industry and Surface Chemistry Group, Symp. Proc. on Particle growth in suspension, Brunel Univ., London, **1972**.
38. Yadav, B. C.; Srivastava R.; Dwivedi, C.D. *Synth. React. in Inorg. Metal-Org. Nano-Metal Chem.* **2007**, *37*, 417.
DOI: 10.1080/15533170701465937
39. Shimizu, Y.; Arai, H.; Seiyama, T. *Sens. Actuators B* **1985**, *7*, 11.
DOI:10.1016/0250-6874(85)87002-5
40. Everett, D; Haynes**,** J. Edt. By D. Everett, vol.1, *The Chemical Society*, London, U.K., **1973**, pp. 131-136.
41. Voigt, E. M.; Tomlinson, R. H. *Can. J. Chem. Rev. Can. Chim.* **1955**, *33*, 215.
42. Traversa, E. Sens. Actuators B 1995, 23, 135.
DOI: 10.1016/0925-4005(94)01268-M
43. Chen, Z.; Lu, C. Sens. Lett. 2005, 274.
DOI:10.1166/sl.2005.045
44. Srivastava, R.; Yadav, B. C.; Dwivedi C. D.; Kumar, R. *Sens. Trans. J*. **2007**, *80*, 1295.

